

Rotational and Vibrational Nonequilibrium Effects in Rarefied Hypersonic Flow

Iain D. Boyd*

Eloret Institute, Palo Alto, California 94303

Results are reported for an investigation into the methods by which energy transfer is calculated in the direct simulation Monte Carlo (DSMC) method. Description is made of a recently developed energy exchange model that deals with the translational and rotational modes. A new model for simulating the transfer of energy between the translational and vibrational modes is also explained. This model allows the vibrational relaxation time to follow the temperature dependence predicted by the Landau-Teller theory at moderate temperatures. For temperatures in excess of about 8000 K, the vibrational model is extended to include an empirical result for the relaxation time. The effect of introducing these temperature-dependent collision numbers into the DSMC technique is assessed by making calculations representative of the stagnation streamline of a hypersonic space vehicle. Both thermal and chemical nonequilibrium effects are included, and the flow conditions have been chosen such that ionization and radiation may be neglected. The introduction of these new models is found to significantly affect the thermal nonequilibrium observed in the flowfield. Larger and more widely ranging differences in the results obtained with the different energy exchange probabilities are found when a significant amount of internal energy is included in the calculation of chemical nonequilibrium.

Nomenclature

C_H	= heat transfer coefficient
\bar{c}	= average molecular velocity
$f(g)$	= relative velocity distribution function
g	= relative velocity of collision
g^*	= characteristic velocity
m_r	= reduced mass of collision
n	= number density
T	= translational temperature
T^*	= characteristic temperature for Z_R
T_{ref}	= reference temperature for variable hard sphere model
VHS	= variable hard sphere
X_i	= mass fraction for species i
Z_R	= rotational collision number
$(Z_R)_\infty$	= infinite temperature collision number
Z_t	= translational collision number
ν	= molecular collision rate
σ_{ref}	= reference collision cross section for VHS model
σ_v	= effective excitation cross section
τ_{LT}	= Landau-Teller vibrational relaxation time
τ_P	= Park's empirical correction for relaxation time
τ_v	= total vibrational relaxation time
ϕ_R	= probability of rotational energy exchange
ϕ_v	= probability of vibrational energy exchange
ω	= parameter in VHS model

Introduction

THE direct simulation Monte Carlo method (DSMC) developed by Bird¹ is an important numerical technique for the calculation of low-density flowfields. The method simulates the flow at the molecular level by calculating collisions on a probabilistic basis. One of the most important aspects of DSMC calculations is the ability to model thermal

nonequilibrium in which the distributions associated with the various energy modes of the gas are not in their equilibrium state. In order to reduce computational overheads, such phenomena are usually modeled in a simplistic manner in which the probability of energy exchange between these various modes is a constant for each type of transfer mechanism. If a particular collision is accepted for internal energy transfer, then postcollision values are sampled from the local equilibrium distribution function in accordance with the Larsen-Borgnakke phenomenological model.²

By employing this energy exchange scheme, significant degrees of thermal nonequilibrium have been calculated for expansions in plumes^{3,4} and for compressions in shock waves.^{5,6} Recently, one of the most interesting applications of the DSMC technique has been to the flowfield surrounding a hypersonic space vehicle such as the Space Shuttle or an aero-assisted space transfer vehicle (ASTV) as described in Refs. 5 and 6. The thermal nonequilibrium in such energetic flows can have a significant impact on the amount of chemical activity and on the convective and radiative heat load to the vehicle. It is therefore of great importance that the models employed in the calculation of energy transfer be physically realistic. For ASTV calculations, the probabilities assumed for rotational and vibrational energy exchange are usually taken to be 0.2 and 0.02, respectively. The value for the transfer of rotational energy has been derived from experimental studies for temperatures of about 1000 K. In the case of vibrational energy exchange, the probability of 0.02 is an estimate of the maximum possible. In reality, the probability of energy transfer would be expected to be much smaller except at very high temperatures.

A variable vibrational exchange probability has been introduced into DSMC calculations by Olynick et al.⁷ by calculating the translational temperature at each cell in the simulation and then employing continuum expressions to evaluate the relaxation time. The problem with this procedure is that the definition of temperature in nonequilibrium conditions is uncertain. The aim of the present work is to introduce a variable exchange probability by deriving a function that may be expressed in terms of a collisional quantity such as the relative velocity. This has previously been performed by Bird for chemical reactions⁸ in which the chemical rate constants are converted into steric factors, which are described as a func-

Presented as Paper 89-1880 at the 20th Fluid Dynamics, Plasma Dynamics, and Lasers Conference, Buffalo, NY, June 12-14, 1989; received Aug. 10, 1989; revision received Nov. 28, 1989. Copyright © 1990 by the American Institute of Aeronautics and Astronautics, Inc. All rights reserved.

*Research Scientist. Member AIAA.

tion of the total collision energy. A similar procedure is adopted here for both the rotational and vibrational energy exchange probabilities whereby continuum formulations, given as a function of temperature, are converted into expressions that may be used in the simulation. This is not the same as employing a temperature obtained from the DSMC calculations. The underlying assumption in the analysis is that the DSMC exchange formulation that provides the equilibrium result under equilibrium conditions may be applied to give the nonequilibrium result under nonequilibrium conditions. Ideally, all internal energy transitions should be treated deterministically. However, the introduction of such a concept into DSMC flow calculations is presently well beyond the capabilities of the largest supercomputers. It is therefore proposed that the ideas described below considerably improve the simulation of such phenomenon in the DSMC technique. The effect of introducing such expressions into the DSMC technique is assessed by making one-dimensional calculations along the stagnation streamline for the flow in front of a hypersonic vehicle. First, the methods for calculating the probability of internal energy transfer are described.

Probability of Rotational Energy Transfer

The collision number of an energy mode is the number of collisions required to bring that mode into equilibrium. The following approximate expression for the rotational collision number was obtained by Parker⁹

$$Z_R = \frac{(Z_R)_\infty}{1 + \frac{\pi^{3/2}}{2} \left(\frac{T^*}{T} \right)^{1/2} + \left(\frac{\pi^2}{4} + \pi \right) \frac{T^*}{T}} \quad (1)$$

where T^* is the characteristic temperature of the intermolecular potential, and $(Z_R)_\infty$ is the limiting value. Though Parker's expression is derived from an analysis involving a large number of assumptions, the temperature dependent nature of Eq. (1) is in agreement with the more rigorous treatment of Lordi and Mates,¹⁰ who performed classical trajectory calculations. In the current work, the value of $(Z_R)_\infty$ is chosen so as to obtain the best correspondence between Parker's results and those of Lordi and Mates. To incorporate Parker's continuum formula into the DSMC technique, an expression for the probability of energy transfer must be developed as a function of the relative collision velocity. This expression must reduce to Eq. (1) when integrated over all possible collisions. Such a formulation has been derived in Ref. 11 and is given as

$$\phi_R \frac{(Z_R)_\infty}{Z_i} = 1 + \frac{\Gamma(2-\omega)}{\Gamma(3/2-\omega)} \left(\frac{2kT^*}{m_r g^2} \right)^{1/2} \frac{\pi^{3/2}}{2} + \frac{\Gamma(2-\omega)}{\Gamma(1-\omega)} \left(\frac{2kT^*}{m_r g^2} \right) \left(\frac{\pi^2}{4} + \pi \right) \quad (2)$$

In the derivation of Eq. (2), the variable hard sphere (VHS) collision model of Bird⁸ has been employed in which the molecular collision rate is given by

$$v = \frac{2n\sigma_{\text{ref}}}{\sqrt{\pi}} \Gamma(2-\omega) \left(\frac{2kT}{m_r} \right)^{1/2} \left[(2-\omega) \frac{T_{\text{ref}}}{T} \right]^\omega \quad (3)$$

In a separate set of calculations,¹¹ Eq. (2) was employed in the calculation of a standing shock wave, and the results obtained were found to offer better correspondence to the experimental data than those with $\phi_R = 0.2$. It has been found by Belikov et al.¹² that Parker's formulation appears to give the correct behavior up to about 4000 K. In addition, it has been shown by Lumpkin et al.¹³ that Eq. (1) gives good agreement with experimental shock wave thickness for a

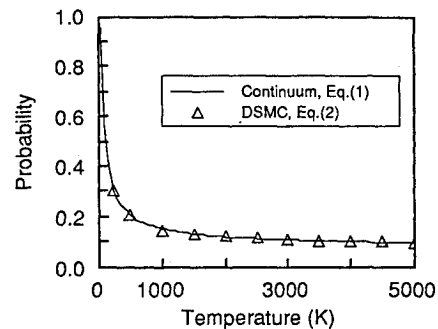


Fig. 1 Rotational energy exchange probability as a function of temperature.

range of Mach numbers. Indeed, in Ref. 13 it is observed that Parker's simple formulation provides better correspondence than the results obtained with calculations that employed a more sophisticated model based on rotational transition rates. As shown in Fig. 1, even at 1000 K the probability of rotational energy transfer for nitrogen is certainly different to 0.2, and the variation in ϕ_R will therefore have some impact on the calculated results. When Eq. (2) is evaluated at each collision, it is found that equipartition of the thermal modes is not achieved. The problem stems from the fact that the collision probability is biased towards those collisions having smaller translational energies. As the Larsen-Borgnakke model assumes local equilibrium and samples postcollision energies from equilibrium distributions, the result of this aspect of the model is to lower the rotational temperature below the required value at equipartition. In the present study, the mean exchange probability for each cell in the computational domain is therefore employed and is obtained by averaging Eq. (2) over all collisions. This procedure leads to the exchange probability at each collision being effectively independent of the instantaneous value and therefore leads to detailed balance as required (see Ref. 11). A further solution to the problem may involve the use of the rotational energy in addition to the translational collision energy. In any case, the use of an averaged exchange probability is still preferable to employing a local temperature in Eq. (1). This is because the definition of temperature is difficult for the nonequilibrium distributions that are present in the flows of interest.

Probability of Vibrational Energy Transfer

In a pure gas of diatomic molecules, the mean probability of vibrational-translational energy exchange may be expressed as

$$\bar{\phi}_v = \frac{1}{\tau_v v} = \int_{-\infty}^{\infty} \phi_v(g) f(g) dg \quad (4)$$

In the following, we wish to choose a form of ϕ_v such that the vibrational relaxation time is given by the expression obtained by Millikan and White,¹⁴ who correlated a number of experimental results. The probability of energy exchange is assumed to be of the form

$$\phi_v = \frac{1}{Z_0} g^* \exp\left(\frac{-g^*}{g}\right) \quad (5)$$

where α and Z_0 are constants, and g^* is a characteristic velocity. The form of Eq. (5) is identical to that originally assumed by Landau-Teller with α set equal to zero. The integral obtained by substituting Eq. (5) into Eq. (4) can only be evaluated approximately using the method of steepest descent.¹⁵ The result obtained with this method reveals that the temperature dependent nature of the vibrational collision

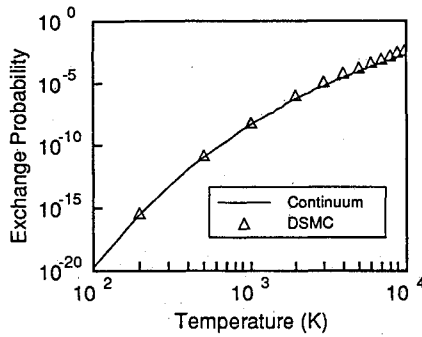


Fig. 2 Vibrational energy exchange probability as a function of temperature.

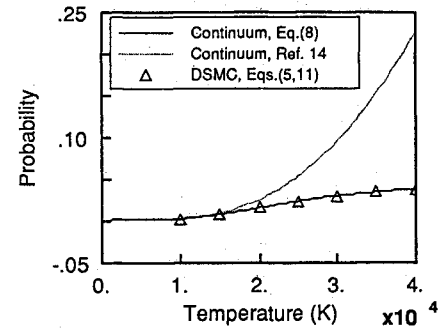


Fig. 3 Vibrational energy exchange probability with Parks empirical correction.

Table 1 Freestream conditions

Altitude, km	U_∞ , km/s	Density, kg/m ³	T_∞ , K	X_{O_2}	X_{N_2}
90	7.5	3.418×10^{-6}	188	0.23	0.77

number is obtained when

$$\alpha = 3 + 2\omega \quad (6)$$

A detailed description of the preceding analysis together with the expressions for the constant Z_0 in Eq. (5) and the characteristic velocity g^* are included in Ref. 15. For a hard sphere interaction ($\omega = 0$), the instantaneous probability of vibrational-translational energy exchange for nitrogen is

$$\phi_v = 1.20 \times 10^{-11} g^3 \exp\left(-\frac{43300}{g}\right) \quad (7)$$

Results obtained with the DSMC technique employing Eq. (7) are plotted in Fig. 2 together with the continuum results. Due to the approximation used in evaluating Eq. (4), the results are not identical and the DSMC results are always less than a factor of 2 above the exact solution.

The vibrational relaxation time of Millikan and White is generally recognized to be valid up to temperatures of about 8000 K. In the consideration of hypersonic flow surrounding space vehicles, the translational temperature may be as high as 40,000 K. To better simulate the vibrational-translational exchange process at such elevated temperatures, Park¹⁶ introduced the following empirical correction

$$\tau_v = \tau_{LT} + \tau_p \quad (8)$$

where τ_{LT} is the Landau-Teller relaxation time and

$$\tau_p = \frac{1}{n\sigma_v \bar{c}} \quad (9)$$

This correction to the vibrational collision number may be evaluated in a similar manner to that employed for rotational-translational energy exchange. If the excitation cross section is taken to be constant, then the following expression is obtained:

$$\phi_p = \frac{\sigma_v}{\sqrt{2}\sigma_{ref}} \frac{1}{\Gamma(2-\omega)} \left[\frac{T}{(2-\omega)T_{ref}} \right]^\omega \quad (10)$$

An expression which reduces to Eq. (10) when integrated over all collisions is

$$\phi_p = \frac{\sigma_v}{\sqrt{2}\sigma_{ref}} \left[\frac{m_r g^2}{2(2-\omega)kT_{ref}} \right]^\omega \quad (11)$$

Table 2 Parameters for rotational energy exchange

Species	$(Z_R)_\infty$	T^* , K	Z_t
N ₂	23.3	91.5	1.5
O ₂	16.5	113.5	1.5
NO	19.5	100.0	1.5

Table 3 Parameters for vibrational energy exchange

Species	Z_0	g^* , m/s	σ_v , m ²
N ₂	8.30×10^{10}	43300	10^{-20}
O ₂	1.50×10^{11}	18200	10^{-20}
NO	1.51×10^{11}	6400	10^{-20}

It should be noted that it is possible to include a temperature dependent form for σ_v if desired. From Eq. (11) it is seen that for hard spheres, the result is independent of the collision velocity. Park's modification to the vibrational relaxation time is implemented in the DSMC method by averaging Eq. (11) over all collisions. To ensure that the integration is being performed correctly, the results for $\omega = 0.25$ and nitrogen molecules are shown in Fig. 3 for the modified vibrational relaxation time of Eq. (8). It is seen that the DSMC and continuum results are in excellent agreement.

Calculations

Having derived expressions that allow both the rotational and vibrational collision numbers to vary with temperature, the effect of introducing these developments into energetic DSMC calculations is now assessed. The problem chosen for consideration is the flow along the stagnation streamline in front of a hypersonic space vehicle. The solution procedure follows that of Bird,¹⁷ who has shown that the stagnation streamline flow may be reduced to one dimension. One end of the computational domain is open through which enter molecules representative of the upstream conditions. At the opposite end is the surface of the space vehicle, which is assumed to be a diffuse reflector with full energy accommodation. As the molecules are reflected back from the wall, a shock wave forms that gradually moves away from the surface. A steady flow is achieved by removing molecules from a downstream portion of the flow with probability proportional

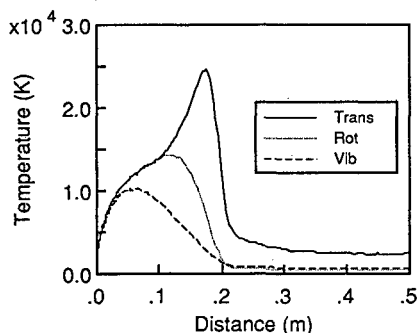


Fig. 4a Thermal nonequilibrium along stagnation streamline for constant exchange probabilities.

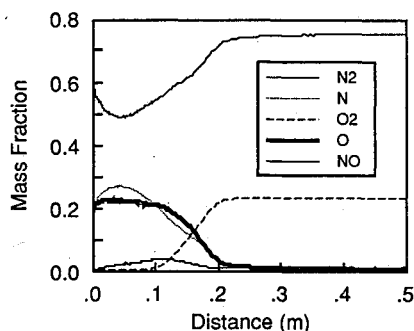


Fig. 4b Species mass fractions along stagnation streamline for constant exchange probabilities.

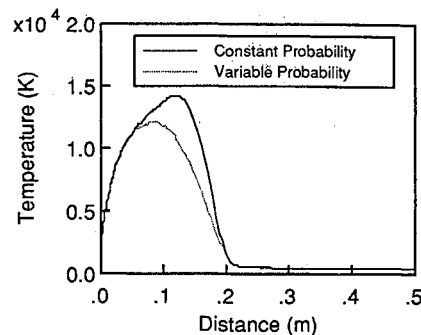


Fig. 5 Comparison of rotational temperature profiles for different rotational energy exchange models.

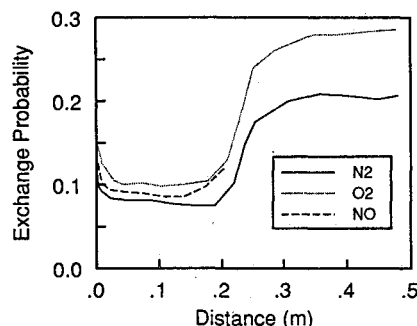


Fig. 6 Variation of rotational energy exchange probabilities.

to the square of the normal velocity component. This procedure has been shown to conserve energy and momentum when the molecules are removed in the region lying between the shock standoff location and the surface.

The conditions investigated represent the exit of the space vehicle through the atmosphere rather than the re-entry. The exit phase is significantly less energetic than re-entry and allows ionization and radiation effects to be omitted from the calculations. An altitude of 90 km has been selected, and the freestream flow conditions are listed in Table 1. The wall-surface temperature is assumed to be constant at 1000 K and is noncatalytic. A five-species gas mixture is employed (N_2 , O_2 , NO , N , O) with 19 different chemical reactions [see Table 2(a), Ref. 18]. Due to the low densities involved, recombination reactions have been omitted from the analysis. Calculations have been completed for three different cases. The first of these follows the previous work by setting $\phi_R = 0.2$ and $\phi_V = 0.02$. Second, the temperature and species-dependent expression in Eq. (2) for rotational-energy transfer is introduced. Finally, both the rotational and the vibrational energy exchange probabilities are calculated as a function of temperature and molecular species using Eq. (2) and Eqs. (6) and (11). Details of the parameters used in the energy exchange models are given in Table 2 for rotation and in Table 3 for vibration. The value for the translational relaxation number Z_t , required in Eq. (2), is that proposed by Fritzsche and Cukrowski.¹⁹

Though the primary focus of the present work is the investigation of thermal nonequilibrium effects, the importance of chemical nonequilibrium cannot be ignored. Initially, rotational energy contributions to the energy available for reaction are only included on a restricted basis, and where required by Bird's steric factor for the VHS model. The fractions of rotational energy allowed to participate in the various reactions are those employed by Bird²⁰ in his general purpose code. The effect of this assumption on the flowfield is also analyzed by allowing all of the rotational energy avail-

able in each collision to be incorporated into the steric factor. For the dissociation reactions it would of course be more realistic to include contributions from the vibrational modes. Unfortunately, the implementation of such a procedure is numerically expensive when Bird's steric factor is employed. It is proposed that the use of the rotational energy will at least give an indication of the importance of including internal energy contributions in the calculation of chemical nonequilibrium.

Results and Discussion

At an altitude of 90 km, Ref. 16 shows that the shock standoff distance, which is defined as the point at which the local density is six times the freestream value, is located at a distance of 0.11 m from the vehicle surface. The present calculations have been performed by forcing the standoff distance to be 0.11 m in each case considered. This procedure assumes that the calculated results are insensitive to the shock standoff location. Investigation of this aspect of the calculations revealed that the exact location did move a small distance in some cases. However, conclusive evidence on this subject requires the simulation of a two-dimensional flow, which lies beyond the scope of the present work. In Fig. 4a, the temperature profiles along the stagnation streamline are plotted for the case in which the probabilities of rotational and vibrational energy exchange are both kept constant. As expected, a significant degree of nonequilibrium exists with the translational mode reaching a peak temperature of about 25,000 K. The results shown offer excellent agreement with the profiles reported in Refs. 5 and 6. The variation along the stagnation streamline of the mass fraction of each of the five species is shown in Fig. 4b for the same case. A significant amount of chemical activity is observed in the flowfield.

Consideration is now given to the effect of introducing a temperature and species-dependent rotational energy exchange probability into the calculations. In Fig. 5 the rotational temperature profiles obtained with the two different

modeling methods are shown. It is found that the maximum rotational temperature attained is significantly reduced for the case of the variable exchange probability. This effect may be explained by examination of Fig. 6 in which the rotational probabilities obtained in the calculations are shown for each of the three molecular species. It may be seen from Fig. 4b that molecular nitrogen dominates the flow; therefore concentration is on this data. At the relatively low freestream temperature, the probability of rotational energy transfer is very close to the nominal value of 0.2 and gradually decreases as the translational temperature increases. It should be noted that the energy exchange probability increases again as the cooling effects of the vehicle surface become important. The values of the exchange probabilities for oxygen are observed to be everywhere greater than those for nitrogen with a maximum of about 0.29 at the freestream boundary. For nitric oxide, a value for the exchange probability is not obtained until a distance of about 0.2 from the vehicle. This is explained by the fact that, up to this point, NO gas exists in insufficient quantities to produce any collisions in the simulation. As the rotational energy exchange probability is quite large at the upstream boundary for both the nitrogen and oxygen molecules, then it might be expected that the rotational temperature in Fig. 4a would lie closer to the translational result at this location. However, Fig. 7 reveals that the various thermal modes are in fact in equilibrium at the upstream location for nitrogen, and this is also found to be the case for the oxygen molecules. Examination of the results obtained for each species revealed that the large translational temperature obtained in Fig. 4a at the upstream boundary is caused by a very small fraction of highly energetic, backscattered atoms and nitric oxide molecules.

In Fig. 8, the vibrational temperature profiles are shown for the two energy exchange probability models. As in the case of rotational relaxation, it is found that the maximum vibrational temperature is significantly reduced. The individual exchange probabilities for each molecular species are plotted in Fig. 9. Careful attention should be given to the labeling of

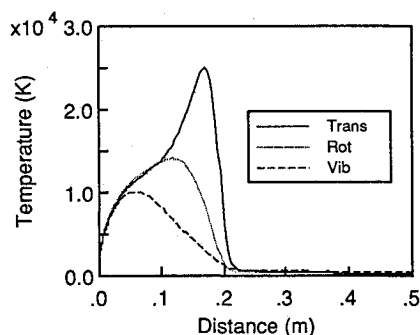


Fig. 7 Thermal nonequilibrium of molecular nitrogen.

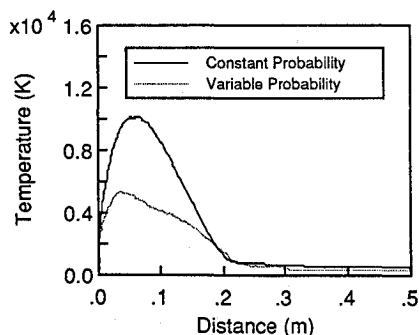


Fig. 8 Comparison of vibrational temperature profiles for different vibrational energy exchange models.

the axes. Only a portion of the domain modeled along the stagnation streamline is included. Beyond distances of about 0.25 m from the vehicle, the collision rate is too low to allow any vibrational energy exchange for the variable probability model. It is to be remembered that the DSMC technique employs a discrete number of simulated molecules in the simulation, which undergo a discrete number of collisions. For calculated exchange probabilities that are very small, e.g., 10^{-4} , it is therefore difficult to accurately resolve the exchange phenomenon. In direct contrast to the results found for the rotational exchange probabilities, the maximum translational temperature gives rise to the maximum exchange probabilities. For both nitrogen and oxygen, these maximum values fall well below 0.02, which is the value previously assumed. It is satisfying to note that the values for nitric oxide lie well above those of the other molecules. This is the trend expected from experiment and shows that such behavior can now be incorporated into the DSMC calculations through application of the variable exchange probability model.

It is therefore found that the introduction of the variable exchange probabilities leads to a greater degree of thermal nonequilibrium in the flow due to the fact that the calculated probabilities are always much smaller than the values of 0.2 and 0.02 normally assumed for energy exchange with the rotational and vibrational modes, respectively. However, at the macroscopic level, only a small effect is observed through the introduction of the temperature dependent models. One example is shown in Fig. 10 where the mass fraction of

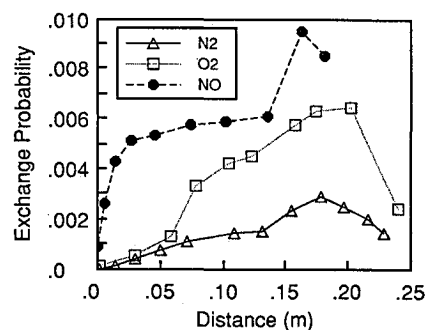


Fig. 9 Variation of vibrational energy exchange probabilities.

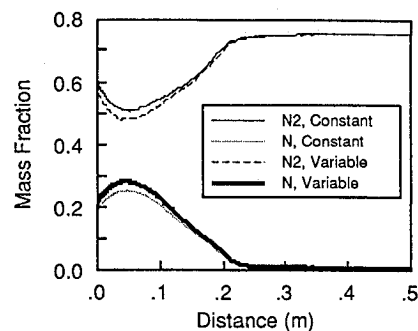


Fig. 10 Comparison of mass fractions of molecular and atomic nitrogen for different energy exchange models.

Table 4 Results for restricted rotational contributions to chemical reactions

ϕ_R	ϕ_v	C_H	Surface mass fraction of N_2
0.2	0.02	0.177	0.561
Eq. (2)	0.02	0.178	0.547
Eq. (2)	Eq. (8)	0.180	0.540

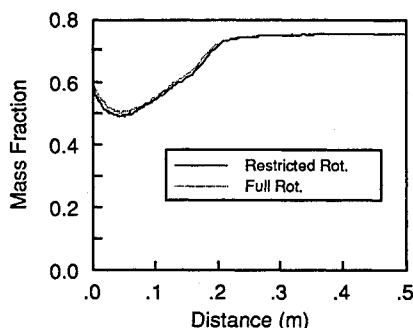


Fig. 11 Comparison of mass fraction of molecular nitrogen for different steric factors.

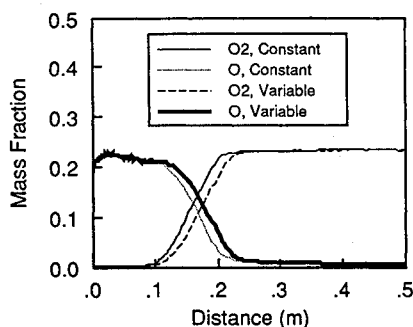


Fig. 12 Comparison of mass fractions of molecular and atomic oxygen for different energy exchange models with full rotational contribution to the steric factor.

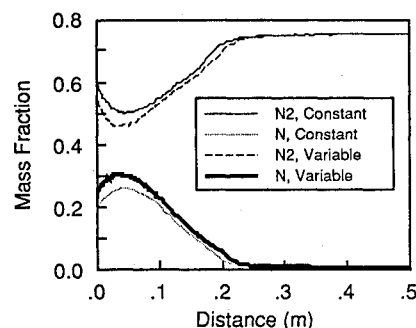


Fig. 13 Comparison of mass fractions of molecular and atomic nitrogen for different energy exchange models with full rotational contribution to the steric factor.

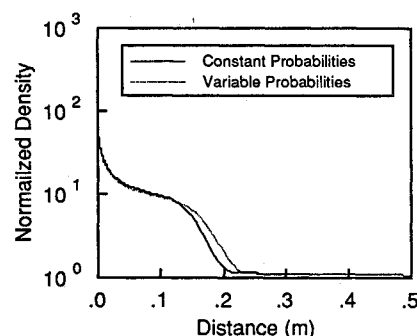


Fig. 14 Comparison of density for different energy exchange models with full rotational contribution to the steric factor.

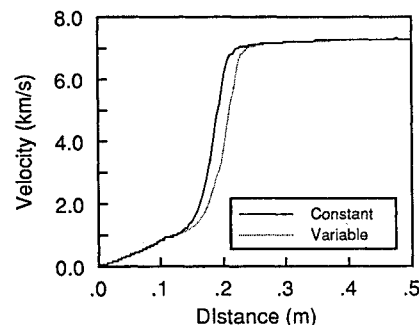


Fig. 15 Comparison of velocity for different energy exchange models with full rotational contribution to the steric factor.

molecular and atomic nitrogen is compared. It is seen that a greater amount of nitrogen atoms is produced in the case where variable probabilities are employed. In Table 4 various results obtained from these simulations are shown. It is found that the heat coefficient increases slightly with the introduction of first the variable rotational exchange probability, and then additionally for the corresponding model for vibration. Simultaneously, the mass fraction of molecular nitrogen that impacts the vehicle surface is reduced.

It is perhaps surprising that the introduction of the new models has had such little effect on the important flow quantities. However, this is almost certainly due to the fact that the internal energy modes are only included in the chemical nonequilibrium phenomenon on a restricted basis. At a time when the significant role of internal energy in chemical nonequilibrium has been incorporated into continuum calculations,^{21,22} it is unsatisfactory for the discrete particle solution methods to lag behind in this area. There is a real requirement for improvement in the modeling of chemical reactions in the DSMC technique. In an attempt to assess the effect of the particular chemical model employed, the same flow conditions have been calculated with the total rotational energy now being available for reaction. In each case where the rotational energy contribution was increased, the reactive cross sections were adjusted so that the effective rates were the same.

In Fig. 11, the mass fraction of molecular nitrogen is shown for the cases where constant exchange probabilities were

employed for both rotational and vibrational energy. It is seen that a reduced amount of dissociation is found for the increased internal energy contribution. This would be expected as Bird's steric factors assume perfect equilibrium for the various thermal modes. Therefore, when the internal temperatures lie below the translational result, which is the case for the flow along most of the stagnation streamline, a smaller rate of reaction will occur.

The thermal nonequilibrium effects discussed above for the restricted rotational energy contribution to chemical reactions

Table 5 Results for different rotational contributions to chemical reactions

Rotational contribution	ϕ_R	ϕ_v	C_H	Surface mass fraction of N_2
Restricted	0.2	0.02	0.177	0.561
Full	0.2	0.02	0.177	0.552
Full	Eq. (2)	0.02	0.182	0.530
Full	Eq. (2)	Eq. (8)	0.188	0.506

were repeated in the new set of calculations. However, larger differences for other flow quantities were discernible. In Fig. 12 are shown the mass fractions for atomic and molecular oxygen for the two cases where constant and variable exchange probabilities were employed. There is a smaller amount of molecular oxygen present in the mixture when the variable models are introduced. Similar behavior is observed for nitrogen, as shown in Fig. 13, but to a lesser extent. The exact explanation for these trends is complicated by the presence of the number of competing reactions that are accounted for in the calculations. The differences between the solutions obtained with the variable exchange probabilities are now large enough to be noticed in such macroscopic quantities as density and velocity, which are plotted in Figs. 14 and 15, respectively. It is found that the density is greater for the variable probability calculations in the region lying between the freestream and the shock standoff location. Thereafter, the variable result is slightly below that obtained with the constant probability. In Fig. 15, it is seen that the velocity solutions obtained with the different methods are clearly different with the variable result lagging behind. These findings are of a similar magnitude to the differences noted by Moss et al. in Ref. 18 for different sets of chemical reaction rate constants. It is therefore found that further uncertainty in such calculations arises from the techniques employed in the simulation of thermal and chemical nonequilibrium effects.

Various global results obtained with these calculations are compared in Table 5 with those previously obtained for the constant exchange probabilities. The assumption of a full rotational energy contribution for chemical reactions results in an increased effect through the inclusion of the variable energy exchange probability models. Once again the heat-transfer coefficient is progressively increased, and the mass fraction of molecular nitrogen at the surface is significantly decreased as the variable exchange probabilities are introduced.

Concluding Remarks

The calculations reported show that the introduction of temperature and species-dependent, internal-energy exchange probabilities into DSMC calculations can have significant impact on the results obtained. The constant values normally employed for rotational and vibrational energy transfer are generally larger than the values calculated in the simulation. The degree of thermal nonequilibrium is therefore increased due to a reduction in the amount of energy transfer performed. Indeed, the vibrational exchange probabilities obtained for nitrogen are an order of magnitude smaller than the constant value previously assumed.

The differences observed in other flow quantities for the different energy exchange models are found to be largest when the internal modes are allowed to contribute a significant amount of energy to that available for each chemical reaction. In the current investigation, only the rotational energy contribution has been considered and is found to be important. In the case where the total rotational energy is included in the collision energy, the variable energy exchange models are found to have a pronounced effect on the heat-transfer coefficient.

It is concluded that consideration should be given to the implementation of the energy transfer probabilities described in this paper. It is probable that the effects observed in the present calculations will be more pronounced for the more energetic flowfields associated with atmospheric re-entry of an ASTV or Mars return vehicles. It is a requirement for the future to investigate such conditions and to consider in detail the role of chemical nonequilibrium in such flows. In addition, the role of the variable exchange probabilities in expanding flows, such as that around the aerobrake skirt of an ASTV, should be considered. In such flow, the freezing of the vibrational temperature plays a significant role in the determination of radiation effects.

Acknowledgment

The author gratefully acknowledges the information supplied by J. N. Moss on the one-dimensional calculations previously undertaken at NASA Langley. Support for the author has been provided by NASA Grant NCC2-582.

References

- ¹Bird, G. A., *Molecular Gas Dynamics*, Clarendon Press, Oxford, England, UK, 1976.
- ²Borgnakke, C., and Larsen, P. S., "Statistical Collision Model for Monte Carlo Simulation of Polyatomic Gas Mixtures," *Journal of Computational Physics*, Vol. 18, 1975, pp. 405-420.
- ³Hueser, J. E., Melfi, L. T., Bird, G. A., and Brock, F. J., "Rocket Nozzle Lip Flow by Direct Simulation Monte Carlo Method," *Journal of Spacecraft and Rockets*, Vol. 23, No. 4, 1986, pp. 363-367.
- ⁴Boyd, I. D., and Stark, J. P. W., "Assessment of Impingement Effects in the Isentropic Core of a Small Satellite Control Thruster Plume," *Proceedings of the Institution of Mechanical Engineers*, Vol. 203, 1989, pp. 97-103.
- ⁵Moss, J. N., and Bird, G. A., "Direct Simulation of Transitional Flow for Hypersonic Reentry Conditions," *Progress in Astronautics and Aeronautics: Thermal Design of Aeroassisted Orbital Transfer Vehicles*, edited by H. F. Nelson, Vol. 96, AIAA, New York, 1985, pp. 113-139.
- ⁶Dogra, V. K., Moss, J. N., and Simmonds, A. L., "Direct Simulation of Stagnation Streamline Flow for Hypersonic Reentry," AIAA Paper 87-0405, Jan. 1987.
- ⁷Olynick, D., Moss, J. N., and Hassan, H., "Influence of Afterbodies on AOTV Flows," AIAA Paper 89-0311, Jan. 1989.
- ⁸Bird, G. A., "Monte Carlo Simulation in an Engineering Context," *Progress in Astronautics and Aeronautics: Rarefied Gas Dynamics*, edited by S. S. Fisher, Vol. 74, Pt. I, AIAA, New York, 1981, pp. 239-255.
- ⁹Parker, J. G., "Rotational and Vibrational Relaxation in Diatomic Gases," *Physics of Fluids*, Vol. 2, No. 4, 1959, pp. 449-462.
- ¹⁰Lordi, J. A., and Mates, R. E., "Rotational Relaxation in Non-polar Diatomic Gases," *Physics of Fluids*, Vol. 13, No. 2, 1970, pp. 291-308.
- ¹¹Boyd, I. D., "Rotational-Translational Energy Transfer in Rarefied Nonequilibrium Flows," *Physics of Fluids A*, Vol. 2, No. 3, 1990, pp. 447-452.
- ¹²Belikov, A. E., Sharafutdinov, R. G., and Sukhinin, G. I., "Nitrogen Rotational Relaxation Time Measured in Free Jets," *Progress in Astronautics and Aeronautics: Rarefied Gas Dynamics*, edited by E. P. Muntz, D. Weaver, and D. H. Campbell, Vol. 117, AIAA, Washington, DC, 1989, pp. 40-51.
- ¹³Lumpkin, F. E., Chapman, D. R., and Park, C., "A New Rotational Relaxation Model for Use in Hypersonic Computational Fluid Dynamics," AIAA Paper 89-1737, June 1989.
- ¹⁴Millikan, R. C., and White, D. R., "Systematics of Vibrational Relaxation," *Journal of Chemical Physics*, Vol. 39, No. 12, 1963, pp. 3209-3213.
- ¹⁵Boyd, I. D., "Monte Carlo Study of Vibrational Relaxation Processes," 17th International Symposium on Rarefied Gas Dynamics, Aachen, FGR, July 1990.
- ¹⁶Park, C., "Problems of Rate Chemistry in the Flight Regimes of Aeroassisted Orbital Transfer Vehicles," *Progress in Astronautics and Aeronautics: Thermal Design of Aeroassisted Orbital Transfer Vehicles*, edited by H. F. Nelson, Vol. 96, AIAA, New York, 1985, pp. 511-537.
- ¹⁷Bird, G. A., "Direct Simulation of Typical AOTV Entry Flows," AIAA Paper 86-1310, June 1986.
- ¹⁸Moss, J. N., Bird, G. A., and Dogra, V. K., "Nonequilibrium Thermal Radiation for an Aeroassist Flight Experiment Vehicle," AIAA Paper 88-0081, Jan. 1988.
- ¹⁹Fritzsche, S., and Cukrowski, A. S., "Relaxation of Translational Energy in Perpendicular Directions for Hard Sphere—A Verification of Analytical Results by Computer Simulations," *Acta Physica Polonica*, Vol. A74, No. 6, 1988, pp. 811-819.
- ²⁰Bird, G. A., "General Programs for Numerical Simulation of Rarefied Gas Flows," private communication, G.A.B. Consulting Pty. Ltd., Killara, Australia, 1988.
- ²¹Park, C., "Assessment of a Two Temperature Kinetic Model for Dissociating and Weakly Ionizing Nitrogen," *Journal of Thermophysics and Heat Transfer*, Vol. 2, No. 1, 1988, pp. 8-16.
- ²²Candler, G., "On the Computation of Shock Shapes in Nonequilibrium Hypersonic Flows," AIAA Paper 89-0312, Jan. 1989.